

# Ultralong-range triatomic Rydberg molecules in an electric field

Javier Aguilera Fernández,<sup>1</sup> Peter Schmelcher,<sup>2,3</sup> and Rosario González-Férez<sup>1,\*</sup>

<sup>1</sup>*Instituto Carlos I de Física Teórica y Computacional, and Departamento de Física Atómica, Molecular y Nuclear, Universidad de Granada, 18071 Granada, Spain*

<sup>2</sup>*Zentrum für Optische Quantentechnologien, Universität Hamburg, Germany*

<sup>3</sup>*The Hamburg Center for Ultrafast Imaging, Luruper Chaussee 149, 22761 Hamburg, Germany*

We investigate the electronic structure of a triatomic Rydberg molecule formed by a Rydberg atom and two neutral ground-state atoms. Taking into account the  $s$ -wave and  $p$ -wave interactions we perform electronic structure calculations and analyze the adiabatic electronic potentials evolving from the  $\text{Rb}(n = 35, l \geq 3)$  Rydberg degenerate manifold. We hereby focus on three different classes of geometries of the Rydberg molecules, including symmetric, asymmetric and planar configurations. The metamorphosis of these potential energy surfaces in the presence of an external electric field is explored.

## I. INTRODUCTION

In recent years, ultralong-range Rydberg molecules (ULRM) formed when a ground-state atom is bound to a Rydberg atom have developed into a field of intense research [1–6]. These ultralong-range species, which were predicted theoretically back in 2000 [7], exhibit an exotic binding mechanism based on the low-energy collisions between a Rydberg electron and a ground-state atom. The elastic scattering is typically described by  $s$ - and  $p$ -wave Fermi-type pseudopotentials [8, 9], and leads to the unusual oscillatory behavior of the corresponding adiabatic potential energy curves. The polar (trilobite) molecular states emerging from the near degenerate high angular momentum atomic Rydberg manifold possess a huge dipole moment whereas the non-polar molecular states emerging, e.g., from quantum defect split  $s$ -states exhibit only a minor dipole moment [10]. Their vibrational energies are in the GHz and MHz regimes, respectively [7, 11]. Apart from the Rb ULRMs within the above-mentioned experiments, Cesium blue detuned ULRMs [12] and Strontium ULRMs [13] from divalent atomic systems have been prepared and explored. The detection of the singlet/triplet hyperfine structure and scattering channels has been very recently performed in [14]. Due to the sensitivity of these Rydberg molecules to external fields, their electronic structure, molecular geometry and rovibrational dynamics could be controlled and manipulated easily by using weak static magnetic and electric fields or laser fields [17–20]. Very recently a selective excitation of rovibrational molecular states with a variable degree of alignment and antialignment has been demonstrated experimentally by using a magnetic field [4].

Adding more ground-state atoms to the Rydberg cloud, polyatomic ultralong-range molecules could be formed. However, very little is known about the structure and properties of these species. In Ref. [15] the emphasis was put on the splitting of the energy levels and

the construction of symmetry-adapted orbitals. While a repulsive interaction does not support bound states, it is shown in Ref. [16] that adding a second ground-state atom, a long-range bound triatomic molecule becomes possible. Recently Rydberg trimers and excited dimers bound by quantum reflection have been studied experimentally and theoretically [2]. We note that experimentally the transition from a Rydberg dimer to a Rydberg polyatomic has been achieved by increasing the principal quantum number of the Rydberg state [3].

In the present work, we explore, to our knowledge for the first time, the impact of an external electric field on the electronic structure of a triatomic ultralong-range molecule formed by a Rydberg atom and two neutral ground-state atoms. The two ground-state atoms and the Rydberg core are described as point particles, and we restrict this study to the low-energy regime approximating the interaction between the Rydberg electron and each neutral atom by the Fermi pseudopotential [8, 9]. Compared to previous studies about the electronic structure of these triatomic Rydberg molecules [15, 16], we include both the  $s$ -wave and  $p$ -wave interactions of the Rydberg electron and the ground-state atoms. Our focus is on three different configurations: two collinear and one planar arrangement of the atoms. For the collinear configurations, we consider the symmetric case where the two ground-state atoms are located on different sides of the positively charged Rydberg core and at the same distance from it, see Fig. 1 (a), and an asymmetric case with the atoms being located on the same side of the  $\text{Rb}^+$  core and at different distances, see Fig. 1 (b). We also analyze a planar configuration where the two straight lines connecting the spatial positions of each ground-state atom and the Rydberg core form an angle smaller than  $\pi$ , thereby assuming that the distances of the two ground-state atoms from the Rydberg core are the same, see Fig. 1 (c).

We investigate the molecular states of collinear and planar geometries by analyzing their adiabatic potential curves (APC) and surfaces (APS) within the Born-Oppenheimer approximation, respectively. For the above-mentioned three configurations, we encounter a

---

\* rogonzal@ugr.es

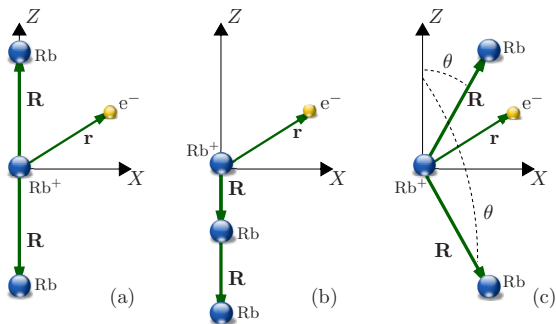


FIG. 1. Sketches (not to scale) of three different configurations of the triatomic molecule formed by a Rydberg atom and two ground-state atoms in the  $XZ$ -plane.

variety of different molecular states with deep potential wells leading to bound ULRMs. We explore in particular the impact of an additional electric field on these adiabatic potentials and show that the bound character of the molecular states increases in case of the linear configuration.

The paper is organized as follows. The Hamiltonian of the triatomic Rydberg molecule in an external electric field is described in Sec. II. We analyze the electronic structure of the linear and planar configurations in Sec. III and Sec. IV, respectively, where we also explore the impact of a static electric field on the corresponding molecular states. The conclusions are provided in Sec. V.

## II. THE MOLECULAR HAMILTONIAN

We consider a triatomic Rydberg molecule formed by a Rydberg atom and two ground-state neutral atoms in a static electric field. It is assumed that the two ground-state atoms and the Rydberg core can be described as point particles and we fix the center of the Laboratory Fixed Frame (LFF) at the position of the ionic core. Our study focuses on the low-energy regime and the interaction between the Rydberg electron and a neutral atom is described by the Fermi pseudopotential [8, 9]:

$$V(\mathbf{r}, \mathbf{R}_i) = 2\pi A_s[k(R_i)]\delta(\mathbf{r} - \mathbf{R}_i) + 6\pi A_p^3[k(R_i)]\overleftarrow{\nabla}\delta(\mathbf{r} - \mathbf{R}_i)\overrightarrow{\nabla} \quad (1)$$

where  $\mathbf{r}$  and  $\mathbf{R}_i = (R_i, \theta_i, \phi_i)$  are the positions of the Rydberg electron and neutral atoms with respect to the Rydberg core, respectively, with  $i = 1, 2$ . The energy-dependent triplet  $s$ - and  $p$ -wave scattering lengths are given by  $A_s(k) = -\tan[\delta_0(k)]/k$  and  $A_p^3(k) = -\tan[\delta_1(k)]/k^3$ , with  $\delta_l(k)$ ,  $l = 0, 1$  being the corresponding phase shifts. The kinetic energy of the Rydberg electron at the collision point with the neutral atom,  $R_i$ , can be approximated by the semiclassical expression  $E_{kin} = k^2/2 = 1/R_i - 1/2n^2$ , with  $n$  being the principal quantum number of the Rydberg electron. The energy-

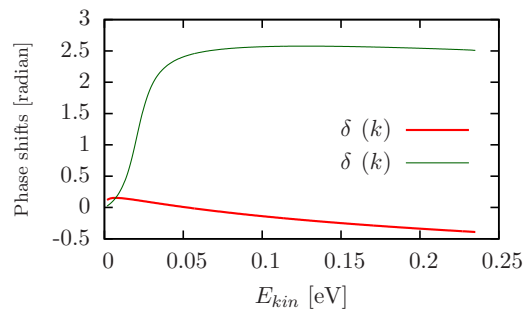


FIG. 2. Energy-dependent triplet phase shifts,  $\delta_0(k)$  and  $\delta_1(k)$ , for the  $s$ - and  $p$ -wave scattering of an electron from the ground-state Rb atom as a function of the electron kinetic energy  $E_{kin}$ .

dependent phase shifts  $\delta_l$  versus the kinetic energy  $E_{kin}$  of the electron are presented in Fig. 2.

The Hamiltonian of this triatomic Rydberg molecule reads

$$H = T_n + H_{el} + V(\mathbf{r}, \mathbf{R}_1) + V(\mathbf{r}, \mathbf{R}_2), \quad (2)$$

where  $T_n$  is the nuclear kinetic energy operator for all relative nuclear motions. The second term stands for the Hamiltonian of the Rydberg electron in an external electric field

$$H_{el} = H_0 + \mathbf{F} \cdot \mathbf{r} = \frac{\mathbf{p}^2}{2m_e} + V_l(r) + \mathbf{F} \cdot \mathbf{r} \quad (3)$$

with  $m_e$  being the electron mass,  $\mathbf{p}$  its relative momentum, and  $V_l(r)$  the angular momentum  $l$ -dependent model potential [21]. The external electric field is taken parallel to the LFF  $Z$ -axis  $\mathbf{F} = F\mathbf{Z}$ , with  $F$  being its field strength.

Within the framework of the Born-Oppenheimer approximation, whose validity is well justified for the ULRM given the typical energy scales of the Rydberg electron as compared to the vibrational states, the total wave function factorizes in two parts that describe the electronic and nuclear motions of the Rydberg trimer. The total wave function can then be written as  $\Psi(\mathbf{r}, \mathbf{R}_1, \mathbf{R}_2) = \psi(\mathbf{r}; \mathbf{R}_1, \mathbf{R}_2)\phi(\mathbf{R}_1, \mathbf{R}_2)$ , where  $\psi(\mathbf{r}; \mathbf{R}_1, \mathbf{R}_2)$  and  $\phi(\mathbf{R}_1, \mathbf{R}_2)$  are the adiabatic electronic and nuclear wave functions, respectively. Note that we focus within this work on the electronic structure of the triatomic ULRM in particular in the presence of an electric field. Thus, the Schrödinger equation for the electronic motion for fixed nuclei is given by

$$[H_0 + \mathbf{F} \cdot \mathbf{r} + V(\mathbf{r}, \mathbf{R}_1) + V(\mathbf{r}, \mathbf{R}_2)]\psi_i(\mathbf{r}; \mathbf{R}_1, \mathbf{R}_2) = \epsilon_i(\mathbf{R}_1, \mathbf{R}_2)\psi_i(\mathbf{r}; \mathbf{R}_1, \mathbf{R}_2) \quad (4)$$

with  $\epsilon_i(\mathbf{R}_1, \mathbf{R}_2)$  being the adiabatic potential energy surface which depends on the position of the two atoms  $\mathbf{R}_1$  and  $\mathbf{R}_2$ . For fixed positions of the ground-state atoms, we solve the adiabatic electronic Schrödinger equation (4) expanding the electronic wave function  $\psi(\mathbf{r}; \mathbf{R}_1, \mathbf{R}_2)$

in the basis formed by the field-free Rydberg electron wave functions  $\chi_{nlm}(\mathbf{r}) = R_{nl}(r)Y_{lm}(\vartheta, \varphi)$ , where  $R_{nl}(r)$  is the radial wave function and  $Y_{lm}(\vartheta, \varphi)$  the spherical harmonics, and  $n$ ,  $l$  and  $m$  are the principal, orbital and magnetic quantum numbers, respectively. Note that  $H_0\chi_{nlm}(\mathbf{r}) = E_{nl}\chi_{nlm}(\mathbf{r})$  with  $E_{nl}$  being the Rydberg electron field-free eigenenergy.

We consider a triatomic Rydberg molecule formed by three rubidium atoms,  $\text{Rb}_3$ , two of them in the ground state and the third one in a Rydberg excited state. Our analysis focuses on the molecular electronic states evolving from the Rydberg degenerate manifold  $\text{Rb}(n = 35, l \geq 3)$ . Thus, to solve the electronic Schrödinger equation (4), we include in the basis set the degenerate manifold  $\text{Rb}(n = 35, l \geq 3)$  and the energetically closest neighboring Rydberg levels  $38s$ ,  $37p$  and  $36d$ . We neglect through the quantum defect of the  $35f$  Rydberg state.

### III. THE LINEAR TRIATOMIC RYDBERG MOLECULE

#### A. The symmetric linear configuration

We start by considering the symmetric linear triatomic ULRM presented in Fig. 1 (a), with the neutral atoms located along the LFF  $Z$ -axis at different sides of the Rydberg core and at the same distance, i. e.,  $R_1 = R_2 = R$  and  $\theta_1 = 0, \theta_2 = \pi$ . This Rydberg molecule has been previously investigated in field-free space by modeling the interaction between the Rydberg electron and the neutral atoms via the  $s$ -wave scattering pseudopotential and neglecting the contribution of the  $p$ -wave scattering [15, 16]. For this triatomic system, the APCs with  $\Sigma$  molecular symmetry (and  $s$ -wave interaction only) are presented in Fig. 3 (a), where the APC of a diatomic ULRM with the ground state atom located on the LFF  $Z$ -axis is also shown. For the triatomic ULRM, we observe that two adiabatic potential curves with gerade and ungerade symmetry split away from the  $\text{Rb}(n = 35, l \geq 3)$  degenerate manifold. In Ref. [15], it is shown that the gerade (ungerade) APC can be written as a sum in terms of the probability densities of Rydberg electronic states with even (odd) angular momentum  $l \geq 3$ . These two APC oscillate around the adiabatic electronic curve of the diatomic ULRM, and, in particular, exhibit deeper potential wells, which indicates a higher degree of stability. At large separations between the atoms and  $\text{Rb}^+$ , these potential curves converge to the APC of a diatomic Rydberg molecule with only one ground-state atom, see Fig. 3 (a), because the sums of even- $l$  and odd- $l$  probability densities that contribute to the gerade and ungerade molecular states, respectively, are very similar as  $R$  increases [15]. Based on previous studies which show that the  $p$ -wave scattering pseudopotential plays a crucial role on the electronic structure of diatomic ULRMs [11, 19, 22], we present here the electronic structure of this triatomic ULRM including both the  $s$  and  $p$ -wave

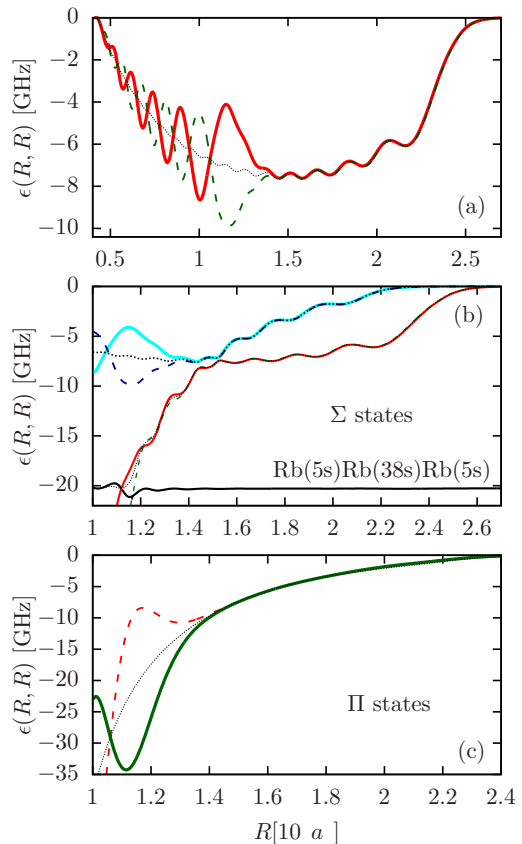


FIG. 3. Symmetric linear triatomic ULRM with the ground-state atoms located along the LFF  $Z$ -axis with  $\theta_1 = 0$  and  $\theta_2 = \pi$ , and at equal separations from the  $\text{Rb}^+$  core, i. e.,  $R_1 = R_2 = R$ . Adiabatic electronic potentials as a function of the distance  $R$  between the Rydberg core and the neutral atoms: (a) obtained including only the  $s$ -wave interaction, (b) and (c) taking into account the  $s$ - and  $p$ -wave interactions and for  $\Sigma$  and  $\Pi$  molecular symmetry, respectively. The gerade and ungerade symmetry curves are plotted with solid and dashed lines, respectively. In panel (b), the APC evolving from the  $\text{Rb}(38s)$  Rydberg state is also shown. For the sake of completeness, we plot the APC of the diatomic ULRM (dotted lines) obtained including (a) only the  $s$ -wave interaction, (b) and (c) both the  $s$ - and  $p$ -wave interactions and for  $\Sigma$  and  $\Pi$  molecular symmetry, respectively. The zero energy has been set to the energy of the field-free  $\text{Rb}(n = 35, l \geq 3)$  degenerate manifold.

interactions of the Rydberg electron and the ground-state atoms. The molecular electronic potentials with  $\Sigma$  and  $\Pi$  symmetry of the triatomic ULRM are shown in Figures. 3 (b) and (c), respectively. For the sake of comparison, the APCs of a diatomic ULRM with the ground state atom located on the LFF  $Z$ -axis are also presented.

Let us first analyze the  $\Sigma$  molecular levels. For the triatomic ULRM, the  $p$ -wave interaction provokes that two additional potentials with  $\Sigma$  molecular symmetry are shifted away from the  $\text{Rb}(n = 35, l \geq 3)$  degenerate manifold. The resonance of the  $p$ -wave scattering length at  $R \approx 780 a_0$  significantly affects the APC and

their slope becomes pronounced for  $R \lesssim 1200 a_0$ . Indeed, two of these APCs suffer avoided crossings with the adiabatic state evolving from the non-degenerate Rydberg level  $\text{Rb}(38s)$ , whose energy, on the scale of the figure, remains approximately constant for larger values of  $R$ . The  $p$ -wave and  $s$ -wave dominated  $\Sigma$ -APCs suffer several avoided crossings close to the internuclear distance  $R \approx 1500 a_0$ . The oscillatory behavior of these adiabatic potentials is due to the highly oscillatory character of the Rydberg electron wave function in the  $\text{Rb}(n = 35, l \geq 3)$  state. The ground-state atoms, considered to a good approximation as point particles, probe locally in space the electronic wave function of the highly excited Rydberg atom. At large separations between the Rydberg core and the ground-state atoms, the  $s$ -wave ( $p$ -wave) dominated  $\Sigma$  molecular states become degenerate and converge to the  $s$ -wave ( $p$ -wave)  $\Sigma$ -APC of the diatomic ULRM. For these large values of  $R$ , the electronic structure of the triatomic ULRM is composed of the molecular states of two diatomic ULRMs that share the same Rydberg core and one has the ground-state atom at  $\theta = 0$  whereas the other one has it at  $\theta = \pi$ .

We focus now on the APCs with  $\Pi$  molecular symmetry. The  $p$ -wave interaction is responsible for the adiabatic potentials with  $\Pi$  molecular symmetry, cf. Fig. 3 (c). In contrast to the  $\Pi$  molecular levels of the diatomic ULRM, these two APCs show potential wells that could accommodate several vibrational bound states. For large internuclear distances, these two adiabatic electronic potentials become degenerate and equal to the corresponding potentials of a diatomic ULRM.

Due to their large dipole moments, Rydberg atoms are extremely sensitive to weak static electric fields, and, as consequence, the level structure of the ULRM is also significantly affected. In Fig. 4 (a), (b) and (c), we present the APCs with  $\Sigma$  molecular symmetry in a static electric field of strength  $F = 100 \text{ V/m}$ ,  $300 \text{ V/m}$ , and  $500 \text{ V/m}$ , respectively. Due to the interaction with the dc field, additional molecular states are shifted from the field-free  $\text{Rb}(n = 35, l \geq 3)$  Rydberg manifold, which reflects that the Stark interaction couples states with field-free orbital numbers  $l$  and  $l \pm 1$ . The electric field couples the adiabatic electronic states with gerade and ungerade symmetry and the degeneracy at large internuclear distances of these APCs is lifted. For  $F = 100 \text{ V/m}$ , the overall energy of one of the states with  $s$ -wave ( $p$ -wave) dominated character decreases, whereas the energy of the second one increases approaching the adiabatic electronic states from the  $\text{Rb}(n = 35, l \geq 3)$  manifold. By further increasing  $F$ , the energies of all APCs show a decreasing behaviour. For  $F = 500 \text{ V/m}$ , two of the APCs are merged with the field-dressed adiabatic electronic potentials that are split from the field-free  $\text{Rb}(n = 35, l \geq 3)$  Rydberg manifold, and we encounter several avoided crossings, see Fig. 4 (c). Thus, only two molecular states remain energetically well separated from the field-dressed levels evolving from the  $\text{Rb}(n = 35, l \geq 3)$  Rydberg manifold. The avoided crossing between the lowest-lying APCs from the Rydberg

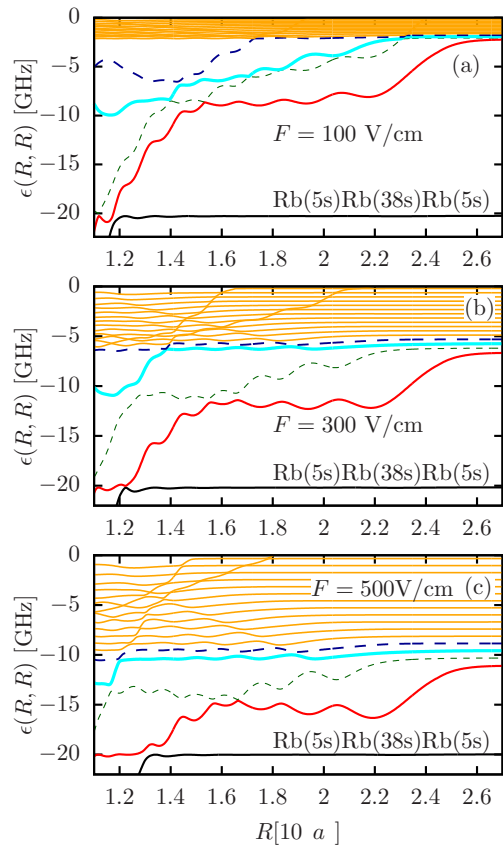


FIG. 4. For the symmetric linear ULRM: molecular states with  $\Sigma$  symmetry evolving from the degenerate manifold  $\text{Rb}(n = 35, l \geq 3)$  versus the interatomic distance  $R$  of the ground-state atoms from the Rydberg core in an external electric field of strength (a)  $F = 100 \text{ V/m}$ , (b)  $F = 300 \text{ V/m}$ , and (c)  $F = 500 \text{ V/m}$ . The APCs have been derived including both the  $s$ -wave and  $p$ -wave interaction. The zero energy has been set to the energy of the field-free  $\text{Rb}(n = 35, l \geq 3)$  degenerate manifold.

trimer  $\text{Rb}(5s)\text{Rb}(n = 35, l \geq 3)\text{Rb}(5s)$  and the molecular state from  $\text{Rb}(5s)\text{Rb}(38s)\text{Rb}(5s)$  becomes broader as  $F$  is increased. Note that due to the quadratic Stark shift of the  $38s$  Rydberg state, the APC of  $\text{Rb}(5s)\text{Rb}(38s)\text{Rb}(5s)$  is very weakly affected by the electric field. Due to the interplay between the interaction of the Rydberg atom with the two neutral atoms and with the external electric field, the change in energy of the APCs depends on the internuclear separation between the Rydberg core and the two ground-state atoms. At large internuclear distances, when the interaction with the two ground-state atoms becomes negligible, all the APCs from the  $\text{Rb}(n = 35, l \geq 3)$  Rydberg manifold are shifted linearly in energy with the dc field strength, which corresponds with the Stark shift of the  $(n = 35, l \geq 3)$  Rydberg manifold of an isolated Rb atom.

Analogous results are found for the field-dressed molecular states with  $\Pi$  molecular symmetry, see Fig. 5. For large internuclear separations  $R \gtrsim 1400 a_0$ , the degen-

eracy of the two  $\Pi$  adiabatic electronic states is lifted. For  $F = 100$  V/m, one of the APCs increases in energy compared to its field-free value, whereas the other one decreases, see Fig. 5 (a), whereas for  $F = 300$  V/m and  $F = 500$  V/m the energies of all APCs are reduced. In addition, the crossing of the field-free APCs at  $R \approx 1060 a_0$  becomes an avoided crossing in the presence of the dc field. These  $\Pi$  molecular states are weakly affected by the external field for  $1000 a_0 \lesssim R \lesssim 1250 a_0$ , their Stark shifts depend quadratically on the field strength and are hardly visible on the scale of Fig. 5. For instance, the energy of the minimum appearing at  $R \approx 1115 a_0$  for the lowest lying  $\Pi$ -APC is shifted 0.3 GHz from its field-free value for  $F = 500$  V/m. As  $F$  is increased, the field-free highest-lying APC gets mixed with the additional field-dressed APCs evolving from the  $\text{Rb}(n = 35, l \geq 3)$  manifold suffering several avoided crossings with them. Again, at large internuclear distances, the Stark shifts of all the APCs from the  $\text{Rb}(n = 35, l \geq 3)$  Rydberg manifold depend linearly on  $F$ .

### B. The non-symmetric linear configuration

We consider now a linear triatomic Rydberg molecule with the two ground-state atoms located along the LFF  $Z$ -axis and at the same side of the Rydberg core, i.e.,  $\theta_1 = \theta_2 = \pi$ . A sketch of this configuration is presented in Fig. 1 (b). The position of one of the atoms is fixed at the  $R_1 = 1200 a_0$ , whereas the distance of the second one from the  $\text{Rb}^+$  core,  $R_2$ , varies for  $R_2 > R_1$ . This condition allows us to neglect the interaction between both ground-state atoms because their vibrational wave functions don't overlap in space. Note that the distance of the first atom from the  $\text{Rb}^+$  core has been arbitrarily fixed to  $R_1 = 1200 a_0$ , and that qualitatively similar results are obtained for other values of  $R_1$ . The  $\Sigma$  and  $\Pi$  molecular states are plotted versus the internuclear separation  $R_2$  in Fig. 6 and Fig. 7, respectively. For the electronic structure with  $\Sigma$  molecular symmetry, the presence of the second atom provokes that two extra adiabatic electronic states are split away from the  $\text{Rb}(n = 35$  and  $l \geq 3)$  degenerate manifold. These two APCs show an oscillatory behaviour superimposed to a broad potential well over the regions  $1400 a_0 \lesssim R_2 \lesssim 2350 a_0$  and  $1300 a_0 \lesssim R_2 \lesssim 2700 a_0$  for the  $p$ -wave and  $s$ -wave dominated states, respectively. These APCs can accommodate many vibrational levels, with spacing  $\sim 150$  MHz approximately, some of them having spatial extensions of a few hundreds Bohr radii. Several avoided crossings are encountered between these two adiabatic electronic states, and also between the  $s$ -wave dominated state and the  $p$ -wave dominated state evolving from the Rydberg diatomic molecule. For large values of  $R_2$ , the interaction with the second atom becomes negligible and the triatomic Rydberg molecule becomes an effective diatomic system. In this case, the two energetically lowest  $\Sigma$ -symmetry APCs have the energies of the correspond-

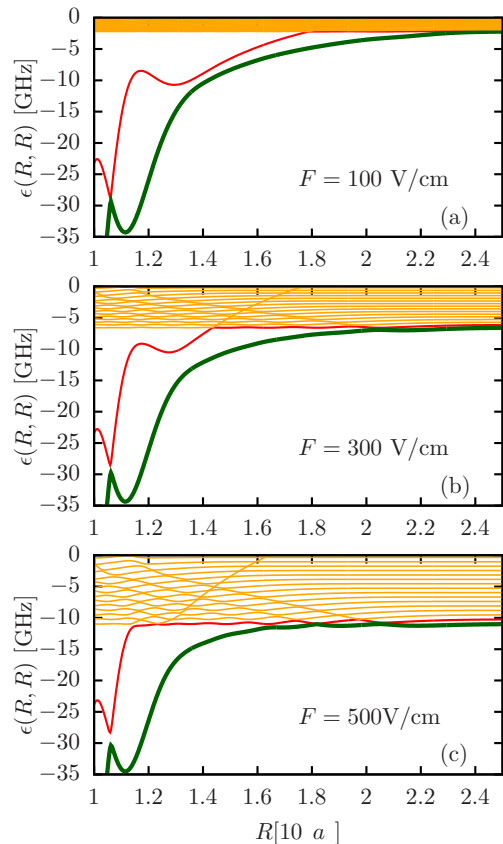


FIG. 5. For the symmetric linear ULRM: electronic states with  $\Pi$  molecular symmetry evolving from the degenerate manifold  $\text{Rb}(n = 35, l \geq 3)$  versus the interatomic distance  $R$  of the ground-state atoms from the Rydberg core in an electric field of strength (a)  $F = 100$  V/m, (b)  $F = 300$  V/m, and (c)  $F = 500$  V/m. The APCs have been derived including both the  $s$ -wave and  $p$ -wave interaction. The zero energy has been set to the field-free energy of the  $\text{Rb}(n = 35, l \geq 3)$  degenerate manifold.

ing electronic states of the diatomic Rydberg molecule with the ground-state atom located at  $R_1 = 1200 a_0$ ; whereas the other two APCs approach zero energy. Due to the second atom, an extra  $\Pi$  molecular state is shifted from the  $\text{Rb}(n = 35$  and  $l \geq 3)$  Rydberg manifold, see Fig. 7 (a), which shows a deep well with a minimum at  $R \approx 1345 a_0$ . This APC is deep enough to accommodate several vibrational bound states, where the triatomic molecule would exist. The lowest-lying molecular state of this symmetry has a shallow potential well of approximately 150 MHz deep at  $R_2 \approx 1410 a_0$ . For  $R \gtrsim 1500 a_0$ , the lowest lying  $\Pi$ -APC shows a constant behaviour with the energy of the corresponding APC of the diatomic ULRM.

In the presence of an external electric field, the energy of the APCs with  $\Sigma$  and  $\Pi$  molecular symmetries decreases as  $F$  is increased, see Fig. 6 and Fig. 7. We start analyzing the results for the electronic states with  $\Sigma$  molecular symmetry. The APC of the

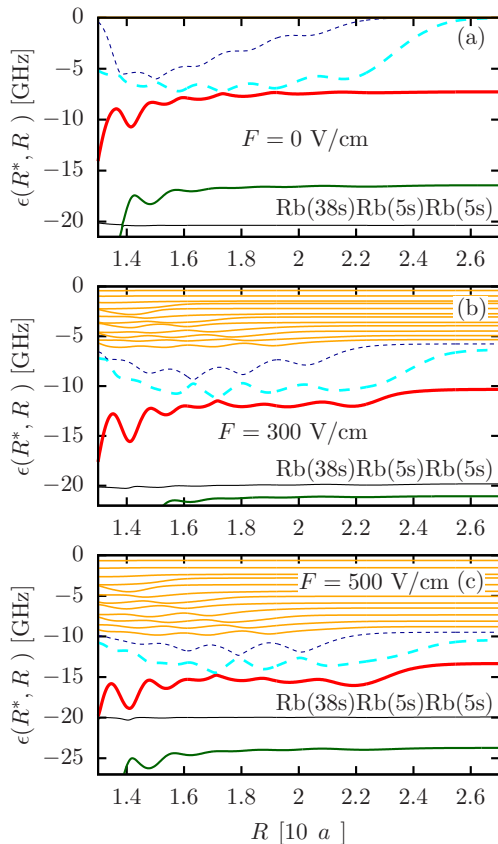


FIG. 6. Asymmetric linear ULRM with the two ground-state atoms located at the same side of the Rydberg core, i.e.,  $\theta_1 = \theta_2 = \pi$  and one fixed at  $R_1^* = 1200 a_0$ . APCs with  $\Sigma$  molecular symmetry evolving from the degenerate manifold  $\text{Rb}(n = 35, l \geq 3)$  versus the separation  $R_2$  between the second atom and  $\text{Rb}^+$ , for an electric field of strength (a)  $F = 0$  V/m, (b)  $F = 300$  V/m, and (c)  $F = 500$  V/m. The APCs have been derived including both the  $s$ -wave and  $p$ -wave interaction. The zero energy has been set to the field-free energy of the  $\text{Rb}(n = 35, l \geq 3)$  degenerate manifold.

$\text{Rb}(38s)\text{Rb}(5s)\text{Rb}(5s)$  trimer is weakly affected by the electric field due to the quadratic Stark effect of the  $\text{Rb}(38s)$  Rydberg state. The lowest-lying APC evolving from the  $\text{Rb}(n = 35, l \geq 3)$  manifold has an energy smaller than the  $\text{Rb}(38s)\text{Rb}(5s)\text{Rb}(5s)$  electronic state for  $F = 300$  V/cm and  $500$  V/cm. The second-lowest-lying APC evolving from the  $\text{Rb}(n = 35, l \geq 3)$  manifold also decreases in energy and its outermost well becomes more pronounced and shows an increasing depth as  $F$  is increased. For the two extra adiabatic electronic states with  $\Sigma$  symmetry, which appear due to the second atom, the electric field provokes that their broad wells become less deep whereas the superimposed oscillatory behaviour remains, see Figures 6 (b) and (c). The Stark effect breaks the degeneracy of the field-free degenerate adiabatic electronic states and extra APCs are shifted from the field-free degenerate manifold  $\text{Rb}(n = 35, l \geq 3)$ . These extra molecular levels show an oscillatory behavior for  $R_2 \lesssim 2000 a_0$ , which provokes many avoided crossings

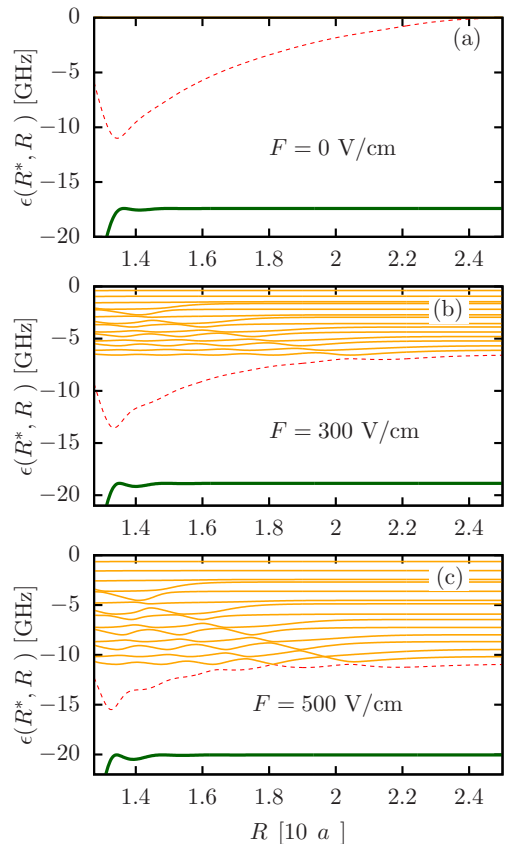


FIG. 7. Asymmetric linear ULRM, with the two ground-state atoms located at the same side of the Rydberg core, i.e.,  $\theta_1 = \theta_2 = \pi$  and one fixed at  $R_1^* = 1200 a_0$ . APCs with  $\Pi$  molecular symmetry evolving from the degenerate manifold  $\text{Rb}(n = 35, l \geq 3)$  as a function of distance  $R_2$  between the Rydberg core and the second atom for an electric field of strengths (a)  $F = 0$  V/m, (b)  $F = 300$  V/m, and (c)  $F = 500$  V/m. The APCs have been derived including both the  $s$ -wave and  $p$ -wave interaction. The zero energy has been set to the field-free energy of the  $\text{Rb}(n = 35, l \geq 3)$  degenerate manifold.

among them, and for larger values of  $R_2$ , they possess a constant energy approximately.

Similar results are observed for the adiabatic energies with  $\Pi$  molecular symmetry, see Fig. 7. The lowest-lying molecular state evolving from the  $\text{Rb}(n = 35, l \geq 3)$  Rydberg manifold suffers a quadratic Stark effect and, therefore, is weakly affected by the weak electric field. The second lowest-lying potential decreases in energy as  $F$  increases and the depth of the pronounced wells is significantly reduced, but remains a few GHz deep and can accommodate vibrational bound states. An increasing number of avoided crossings for large values of  $R_2$  with increasing field strength is encountered.

#### IV. THE PLANAR TRIATOMIC RYDBERG MOLECULE

In this section, we consider a planar ULRM with the neutral atoms located in the LFF  $XZ$ -plane, i.e.,  $\phi_1 = \phi_2 = 0$ , and  $\theta_2 = \pi - \theta_1$  with  $0 \leq \theta_1 < \pi/2$ , see Fig. 1 (c). For the sake of simplicity, we restrict this study to the configuration with the ground-state atoms located at the same distance from the Rydberg core, i.e.,  $R_1 = R_2 = R$ . Note that we impose the conditions  $0 \leq \theta_1 < \pi/2$  and  $\pi/2 < \theta_2 \leq \pi$  to avoid the spatial overlap of the vibrational states of the two ground-state atoms, such that the interaction between them can be neglected. The two energetically lowest lying APS evolving from the Rb( $n = 35, l \geq 3$ ) Rydberg manifold are shown as a function of  $R$  and  $\theta_1$  in Fig. 8.

The field-free APS shows a weak dependence on the polar angle  $\theta_1$  for different values of  $R$ , cf. Fig. 8 (a). For  $R \gtrsim 2000 a_0$ , these field-free APSs are almost independent of the angle  $\theta_1$ , whereas for smaller internuclear separations, we encounter a smooth dependence on  $\theta_1$  for  $\theta_1 \gtrsim 0.8$ . This is due to the spatial proximity of the two ground-state atoms. By adding an electric field, the APS strongly depends on the polar angle  $\theta_1$ . The electric field parallel to the  $Z$  axis favours the linear configuration of the ULRM with both ground-state atoms located along the  $Z$  axis, see Figures 8 (b) and (c). For this APS, the deepest well is shifted towards larger values of  $R$  as  $F$  is increased, and it is located at  $R \approx 2200 a_0$ ,  $\theta_1 = 0$  and  $\theta_2 = \pi$  for  $F = 500$  V/m. This molecular curve approaches to a constant energy, given by the corresponding Rydberg state of the field-dressed Rb for large internuclear separations and large values of  $\theta_1$ . For  $F = 500$  V/m, this effect is observed for  $\theta_1 \gtrsim 1.1$ , and its limit is the energy the lowest-lying field-dressed state of the Rydberg manifold ( $n = 35, l \geq 3$ ) of an isolated Rb atom in an electric field.

#### V. CONCLUSIONS

We have investigated ultralong-range triatomic Rydberg molecules formed by a Rydberg rubidium atom and two ground-state Rb atoms in the presence of an external electric field. This is, to our knowledge, the first investigation of such a triatomic ULRM in an electric field. The symmetric and asymmetric linear configurations, as

well as a planar one with the neutral atoms located at the same distance from the Rydberg core have been explored. We have performed an analysis of the electronic structure for the Rb Rydberg atom in the degenerate manifold ( $n = 35, l \geq 3$ ). For the linear configurations, in the absence of the electric field several molecular states, with  $\Sigma$  and  $\Pi$  symmetry, are split from the Rb( $n = 35, l \geq 3$ ) manifold, showing an oscillatory behaviour with many wells accommodating vibrational levels where the Rydberg molecule would exist. For the planar configuration, we encounter that the molecular states only show a significant dependence on  $\theta_1$  and  $\theta_2$  as the two ground-state atoms approach each other. The electric field favours the symmetric linear configuration and strengthens the bound state character of molecular states, and vibrational states with the spatial extensions of a few hundreds Bohr radii could appear.

An immediate extension of this work would be to investigate the electronic structure and vibrational properties of an ultralong-range triatomic molecule formed from a Rb Rydberg atom in a non-degenerate state with orbital quantum number  $l \leq 3$ . For diatomic Rydberg molecules, it has been shown that the Rydberg-atom fine structure and the hyperfine coupling of the ground-state atom significantly alter the adiabatic electronic potentials evolving from the Rydberg atom in such excited states [14, 23]. By including these couplings for a triatomic Rydberg molecule, the potential energy surfaces depend on the hyperfine states of the ground-state atoms as well as on the fine structure of the Rydberg atom. As a consequence, the complexity of the molecular states would be significantly enhanced.

#### ACKNOWLEDGMENTS

R.G.F. and J.A.F. acknowledge financial support by the Spanish project FIS2014-54497-P (MINECO), and by the Andalusian research group FQM-207. We also acknowledge financial support by the Initial Training Network COHERENCE of the European Union FP7 framework. We would like to thank Markus Kurz and Christian Fey for fruitful discussions.

#### REFERENCES

- 
- [1] V. Bendkowsky, B. Butscher, J. Nipper, J.P. Shaffer, R. Löw and T. Pfau, *Nature* **458**, 1005 (2009)
  - [2] V. Bendkowsky, B. Butscher, J. Nipper, J. B. Balewski, J. P. Shaffer, R. Löw, T. Pfau, W. Li, J. Stanojevic, T. Pohl, and J. M. Rost, *Phys. Rev. Lett.* **105**, 163201 (2010)
  - [3] A. Gaj, A. T. Krupp, J. B. Balewski, R. Löw, S. Hofferberth and T. Pfau, *Nature Comm.* **5**, 4546 (2014)
  - [4] A.T. Krupp, A. Gaj, J.B. Balewski, S. Hofferberth, R. Löw, T. Pfau, M. Kurz, and P. Schmelcher, *Phys. Rev. Lett.* **112**, 143008 (2014)
  - [5] A. Gaj, A.T. Krupp, P. Ilzhöfer, R. Löw, S. Hofferberth, and T. Pfau, *Phys. Rev. Lett.* **115**, 023001 (2015)
  - [6] M. Schlagmüller, T. Cubel Liebisch, H. Nguyen, G. Lockheed, F. Engel, F. Böttcher, K. M. Westphal, K. S. Kleinbach, R. Löw, S. Hofferberth, T. Pfau, J. Pérez-Ríos and

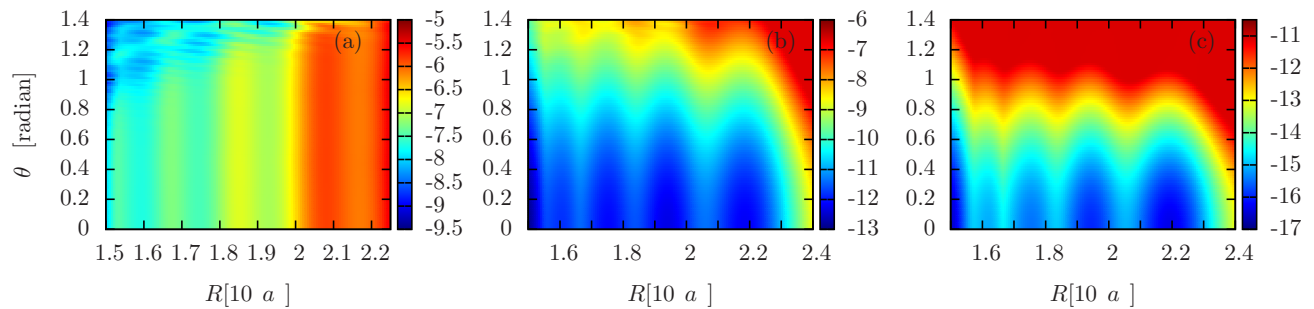


FIG. 8. For the planar ULRM: The lowest lying APS evolving from the Rb( $n = 35$ ,  $l \geq 3$ ) Rydberg manifold in an external electric field parallel to the LFF  $Z$  axis and field strength (a)  $F = 0$  V/m, (b)  $F = 300$  V/m, and (c)  $F = 500$  V/m. The APSs have been derived including both the  $s$ -wave and  $p$ -wave interaction. The zero energy has been set to the field-free energy of the Rb( $n = 35$ ,  $l \geq 3$ ) degenerate manifold.

- C. H. Greene, arXiv:1510.07003 (2015)
- [7] C.H. Greene, A.S. Dickinson, and H.R. Sadeghpour, Phys. Rev. Lett. **85**, 2458 (2000)
- [8] E. Fermi, Nuovo Cimento **11**, 157 (1934)
- [9] A. Omont, J. Phys. **38**, 1343 (1977)
- [10] W. Li, T. Pohl, J.M. Rost, S.T. Rittenhouse, H.R. Sadeghpour, J. Nipper, B. Butscher, J.B. Balewski, V. Bendkowsky, R. Löw and T. Pfau, Science **334**, 1110 (2011)
- [11] E. L. Hamilton, C. H Greene and H. R. Sadeghpour, J. Phys. B **35**, L199 (2002)
- [12] J. Tallant, S.T. Rittenhouse, D. Booth, H.R. Sadeghpour, and J.P. Shaffer, Phys. Rev. Lett. **109**, 173202 (2012)
- [13] B.J. DeSalvo, J.A. Aman, F.B. Dunning, T.C. Killian, H.R. Sadeghpour, S. Yoshida and J. Burgdörfer, Phys. Rev. A **92**, 031403 (2015)
- [14] H. Saßmannshausen, F. Merkt, and J. Deiglmayr, Phys. Rev. Lett. **114**, 133201 (2015)
- [15] I.C.H. Liu and J.M. Rost, Eur. Phys. J. D **40**, 65 (2006)
- [16] I.C.H. Liu, J. Stanojevic, and J.M. Rost, Phys. Rev. Lett. **102**, 173001 (2009)
- [17] I. Lesanovsky, H.R. Sadeghpour, and P. Schmelcher, J. Phys. B **39**, L69 (2007)
- [18] M. Kurz, M. Mayle and P. Schmelcher, Europhys. Lett. **97** 43001 (2012)
- [19] M. Kurz and P. Schmelcher, Phys. Rev. A. **88**, 022501 (2013)
- [20] M. Kurz and P. Schmelcher, J. Phys. B **47**, 165101 (2014)
- [21] M. Marinescu, H. R. Sadeghpour, and A. Dalgarno, Phys. Rev. A **49**, 982 (1994)
- [22] A. A. Khuskivadze, M. I. Chibisov, and I. I. Fabrikant, Phys. Rev. A **66**, 042709 (2002)
- [23] D. A. Anderson, S. A. Miller, and G. Raithel, Phys. Rev. A **90**, 062518 (2014)